JOURNAL OF AIRCRAFT
Vol. 43, No. 6, November–December 2006

Engineering Notes

ENGINEERING NOTES are short manuscripts describing new developments or important results of a preliminary nature. These Notes should not exceed 2500 words (where a figure or table counts as 200 words). Following informal review by the Editors, they may be published within a few months of the date of receipt. Style requirements are the same as for regular contributions (see inside back cover).

Vortex Interactions Between Chined Forebody and Strake

Bao-Feng Ma* and Xue-Ying Deng†
Beijing University of Aeronautics and Astronautics, 100083 Beijing, People's Republic of China

DOI: 10.2514/1.25898

Nomenclature

C_p = surface pressure coefficients, $(p - p_\infty)/(0.5\rho U_\infty^2)$
L = wing root chord length
p_∞ = freestream static pressure
Re = Reynolds number based on the wing root chord, UL/ν
U_∞ = freestream velocity
α = angle of attack
ξ_x = local nondimensional coordinates based on the characteristic length which is the sectional circumference for the sections S1–S8 and the curve length of the sectional upper surface for the sections S9–S19

Subscript

x = pressure-measurement sections index: S1–S19

Introduction

MODERN aircraft are increasing to use a chined forebody for reducing radar cross section (RCS), producing larger lift and gaining better high speed performances. The vortical flow around a chined forebody is relatively stable because its separation lines are fixed at the sharp side-edges [1–3], which is very different from the traditional smoothed-side forebody [4], but resembles the high sweep delta-wing with sharp leading edges [2–5]. Many techniques to controlling the chined-forebody vortices have been adopted to produce the side-force required for the yawing control of aircraft at high angles of attack [6–11]. However, the vortices of the chined forebody not only influence the loads distribution of the forebody itself, but also change the aerodynamic characteristics of other components on aircraft through vortex interactions, e.g., interacting with the wing and strake vortices, etc. Erickson and Brandon [12] have experimentally investigated a chined forebody coupled with a slender delta-wing and identified the mechanisms of the forebody and wing vortical flow. Lemay and Rogers [13] studied the effects of blowing on the chined-forebody and wing vortex interactions, and found a coiling of the wing and chined-forebody vortices would promote vortex breakdown and decoupling of them would delay vortex breakdown. Rao and Puram [14] conducted experimental research to control the interaction of the chined forebody with a delta-wing at high angles of attack through manipulating chined-forebody vortices. Hall [15] has also studied the effects of the interaction between the chined-forebody and wing vortices on the stability of a generic fighter configuration.

As mentioned, some experimental studies have been carried out about the interaction of the chined-body vortices with the wing vortices. But no studies have been done concerning the effect of the strake on the vortex interaction between the chined forebody and wing. The present authors found in experiments that the structure of the vortex system would be significantly changed through the vortex interaction when adding a small strake in front of the wing. The change of the vortical flow would further impact the loads distribution of the wing so as to seriously influence aerodynamic characteristics of the configuration. This note is to present this interesting phenomenon by off-surface flow visualizations and surface pressure measurements.

Experiments Setup

The experiment was conducted in low speed, low noise, and open-circuit wind-tunnel at Fluid Mechanics Institute of Beijing University Aeronautics and Astronautics. The test section of the wind-tunnel is $1.5 \times 1.5 \times 2.5$ m. The freestream turbulence level in the test section is less than 0.1%. A mounting sting supported the model and allowed the angles of attack to be varied from 0 to 90 deg.

The experimental model is made from duralumin and its drawing is shown in Fig. 1. Besides a chined forebody, the model also includes a strake with 72 deg sweep and a wing with 42 deg sweep. The strake and wing is coplanar and located at the upper half part of afterbody. The strake can be removed or added if desired. Pressure taps of 0.8-mm-diam were distributed on the upper and lower surface of the forebody (S1–S8 sections), and the upper surface of the wing (S9–S19 sections). PSI 9816 intelligent pressure scanivalves were connected with the pressure taps through the rubber tubes. Total 32 PSI 9816 modules (512 pressure channels) with full-scale 1 PSI (7 kpa) were equipped and enough for the pressure measurements of the present model.

The steel wires of 0.1-mm-diam were used for smoke flow visualizations and they were distributed on the leading-edge of the wing and the side-edge of the chined forebody but far away from the nose tip. The smoking agent was propanetriol, which can be volatilized smoke fog when the wires were electrified to heat. A 5 W Argon ion laser as the sheet light resource was used for illuminating. The recording device was Sony DSC-V1 digital camera with the resolution of 5.25 million pixels. To know whether the wires would change the vortical flow pattern, the pressure-measurement results were compared before and after the wires were added. It was found that the wires have almost no effects on the results.

The seven repeated pressure measurements based on the strake-wing-body configuration have been carried out at 24.5 deg angle of attack. Based on the seven measurements, it can be obtained the total standard deviation of the pressure coefficients 0.0065, the total uncertainty ± 0.016, and the relative total uncertainty relative to the maximum pressure coefficient 0.66%.

Received 15 June 2006; revision received 20 July 2006; accepted for publication 25 July 2006.

*Postdoctoral Research Assistant, Ministry-of-Education Key Laboratory of Fluid Mechanics; bf-ma@buaa.edu.cn.
†Professor, Ministry-of-Education Key Laboratory of Fluid Mechanics; dengxueying@vip.sina.com. Member AIAA.

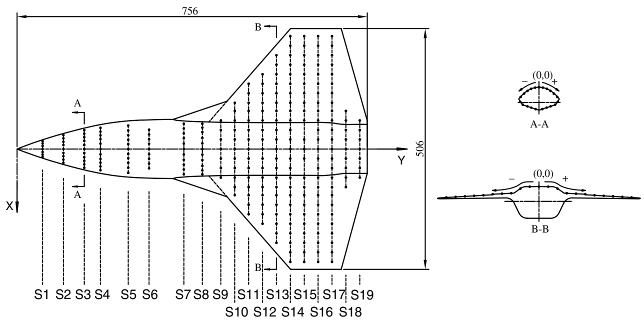

Fig. 1 Experimental model with a chined forebody and strake wing.

Results and Discussion

To determine the effect of the strake on vortex structure of the chined forebody and wing, two configurations were experimentally studied: the wing-body and strake-wing-body configuration, with or without the strake, respectively.

Figure 2 presents the smoke flow visualization results from the front to rear sections for the wing-body (left column) and strake-wing-body (right column) configurations. The Reynolds number for the flow visualization was relatively low, because the freestream velocity cannot be too high to obtain clear smoke flow pictures.

The section S7 is just located at the rear of the strake apex, so the strake vortices can be found besides the forebody vortices for the strake-wing-body configuration. But only a pair of forebody vortex can be found for the wing-body configuration without the strake. At section S12, the forebody vortices of the wing body become stronger and are situated over the afterbody, and the wing vortex was also produced at both sides of the forebody vortex. But for the strake-wing-body, the forebody vortex twists together with the strake vortex and form one concentrated vortex, for simplicity calling it the forebody-strake vortex. Moreover the forebody-strake vortex has moved towards the leading-edge of the wing. With the development of the vortex system towards downstream, the forebody vortex deflects outboard gradually for the wing-body configuration, and for the strake-wing-body configuration, the smoke flow boundary for distinguishing the forebody-strake vortex and the wing vortex become indistinct, as depicted at section S14 and S17 in Fig. 2.

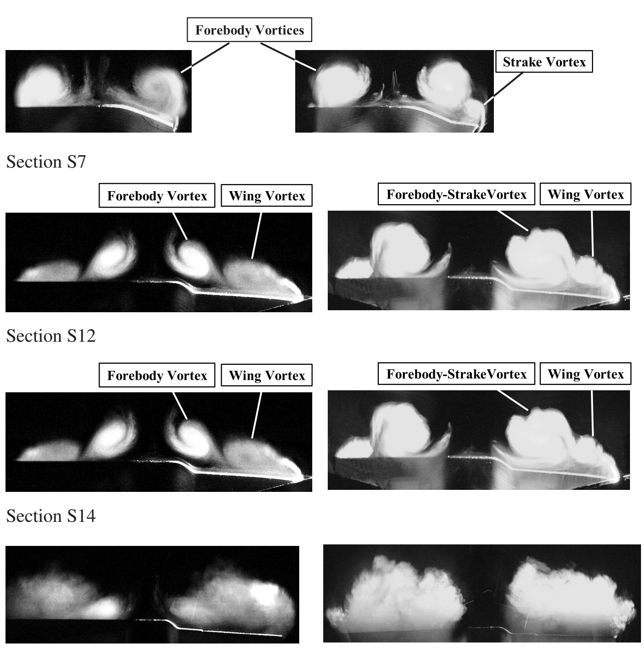

a) Wing-Body b) Strake-Wing-body

Fig. 2 Smoke wires flow visualization photographs, $\alpha = 24.5$ deg, $Re = 1.5 \times 10^5$, from rear view.

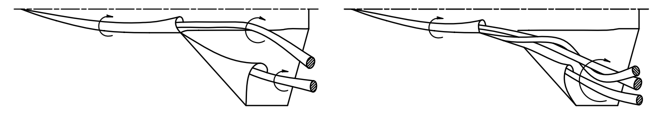

a) Wing-Body b) Strake-Wing-Body

Fig. 3 Schematic diagrams of vortex systems around the wing body and strake-wing body.

The schematic diagrams of the vortex systems around the wing-body and strake-wing-body are, based on the smoke flow visualization results, presented in Fig. 3.

Figure 4 has shown the comparison of the pressure curves at different sections for two configurations to find the vortex interaction effects on the surface loads distribution. The two pressure curves at section S4 were almost of superposition, which indicated that the strake had almost no effect on the forebody vortex and loads distribution before the strake. But after the strake, the pressure distributions for the two configurations were very different. For the wing body, the remarkable suction peaks were induced by the forebody vortices on the afterbody, and the wing vortices also induced suction peaks on the wings of both sides of the afterbody. But for the strake-wing-body, only one suction peak was found. The suction peak on the strake-wing-body was located in the middle of the two ones induced by the forebody vortex and the wing vortex on the wing body, which was the resultant consequence by the forebody-strake vortex and the wing vortex.

The pressure results of section S13 at 19.5 and 29.5 deg angles of attack for two configurations are shown in Fig. 5. The difference of the pressure distributions was similar to the one at 24.5 deg angle of attack.

Because the Reynolds numbers were different for the flow visualization and pressure measurements, the Reynolds numbers effect on the results has been considered by pressure measurements, as shown in Fig. 6. In range of the Reynolds numbers of the present

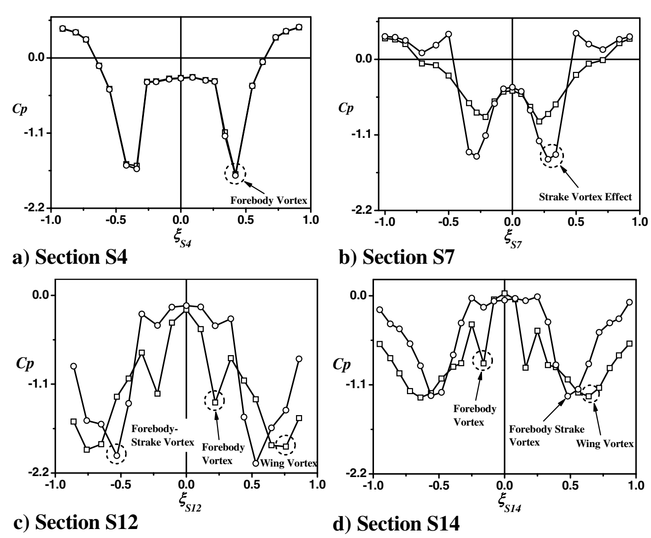

a) Section S4 b) Section S7

c) Section S12 d) Section S14

Fig. 4 Sectional pressure distributions, $\alpha = 24.5$ deg, $Re = 9.0 \times 10^5$, from rear view: □, wing body; ○, strake-wing body.

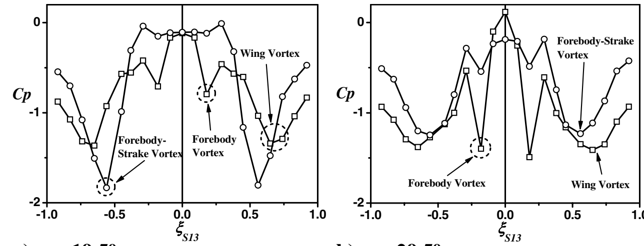

a) $\alpha = 19.5°$ b) $\alpha = 29.5°$

Fig. 5 Section S13 pressure distributions at angles of attack, $Re = 9.0 \times 10^5$, from rear view: □, wing body; ○, strake-wing body.

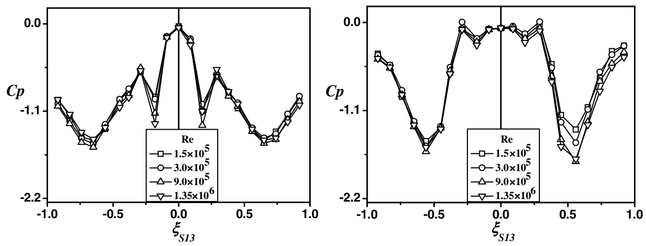

a) Wing-Body **b) Strake-Wing-Body**

Fig. 6 ***Re*** **effects on the pressure distributions, section S13, $\alpha = 24.5$ deg, from rear view.**

experiments, the Reynolds numbers have very little effects on the loads distribution of the configurations.

Conclusions

The vortex system over the chined forebody is greatly influenced at high angles of attack when adding a small strake in front of the wing. The chined-forebody vortex twists together with the strake vortex and forms one forebody-strake vortex and then moves outwards along the wing span. The forebody-strake vortex induces a large suction peak on the wing, which would be beneficial to the lift-enhancement for aircraft. But after adding the strake, it has almost no effects on the vortical flow and loads distribution of the chined forebody before the strake. In range of the Reynolds numbers of the present experiments, the Reynolds numbers have very little effect on the loads distribution of the configurations.

References

[1] Mange, R. L., and Roos, F. W., "The Aerodynamics of a Chined Forebody," AIAA Paper 98-2903, June 1998.

[2] Kegelman, J. T., and Roos, F. W., "Influence of Forebody Cross-Section Shape on Vortex Flowfield Structure at High Alpha," AIAA Paper 91-3250, Sept. 1991.

[3] Lowson, M. V., and Ponton, A. J. C., "Symmetry Breaking in Vortex Flows on Conical Bodies," *AIAA Journal*, Vol. 30, No. 6, 1992, pp. 1576–1583.

[4] Deng, X. Y., Wang, G., Chen, X. R., Wang, Y. K., Liu, P. Q., and Xi, Z. X., "A Physical Model of Asymmetric Vortices Flow Structure in Regular State over Slender Body at High Angle of Attack," *Science in China Series E*, Vol. 46, No. 6, 2003, pp. 561–573.

[5] Stahl, W. H., Mahmood, M., and Asghar, A., "Experimental Investigations of the Vortex Flow on Delta Wings at High Incidence," *AIAA Journal*, Vol. 30, No. 4, 1992, pp. 1027–1032.

[6] Arena, A. S., Nelson, R. C., and Schiff, L. B., "Lateral Control at High Angles of Attack using Pneumatic Blowing Through a Chined Forebody," AIAA Paper 93-3624-CP, 1993.

[7] Boalbey, R. E., Ely, W. L., and Robinson, B. A., "A Sensitivity Study for Pneumatic Vortex Control on a Chined Forebody," AIAA Paper 93-0049, Jan. 1994.

[8] Arena, A. S., Jr., Nelson R. C., and Schiff L. B., "Directional Control at High Angles of Attack Using Blowing Through a Chined Forebody," *Journal of Aircraft*, Vol. 32, No. 3, 1995, pp. 596–602.

[9] Cummings, R. M., Schiff, L. B., and Duino, J. D., "Experimental Investigation of Tangential Slot Blowing on Generic Chined Forebody," *Journal of Aircraft*, Vol. 32, No. 4, 1995, pp. 818–824.

[10] O'Rourke, M., "Experimental Investigation of Slot Blowing for Yaw Control on a Generic Fighter Configuration with a Chined Forebody," AIAA Paper 95-1798, June 1995.

[11] Williams, S. P. and Garry, K. P., "An Experimental Investigation into Yaw Control at Alpha on a Chined Forebody Using Slot Blowing," *The Aeronautical Journal*, Vol. 100, No. 998, Oct. 1996, pp. 355–363.

[12] Erickson, G. E., and Brandon, J. M., "On the Nonlinear Aerodynamic and Stability Characteristics of a Generic Chined-Forebody Slender-Wing Fighter Configuration," AIAA Paper 87-2617, Aug. 1987.

[13] Lemay, S., and Rogers, L., "Pneumatic Vortex Flow Control on a 55-Degree Cropped Delta Wing with Chined Forebody," AIAA Paper 90-1430, June 1990.

[14] Rao, D. M., and Puram, C., "Chine Forebody Vortex Manipulation by Mechanical and Pneumatic Techniques on a Delta Wing Configuration," AIAA Paper 91-1812, June 1991.

[15] Hall, R. M., "Impact of Fuselage Cross Section on the Stability of a Generic Fighter," AIAA Paper 98-2725, June 1998.